Bull. Chem. Soc. Ethiop. **2024**, 38(6), 1625-1638.
DOI: https://dx.doi.org/10.4314/bcse.v38i6.10

ISSN 1011-3924
Printed in Ethiopia
Online ISSN 1726-801X

DESIGN, SYNTHESIS, CHARACTERIZATION, DFT, MOLECULAR DOCKING, AND *IN VITRO* SCREENING OF METAL CHELATES INCORPORATING SCHIFF BASE

Nuha A. Mustafa* and Sahbaa Ali Ahmed*

University of Mosul, College of Science, Department of Chemistry, Ninevah, Iraq

(Received March 26, 2024; Revised June 10, 2024; Accepted June 12, 2024)

ABSTRACT. Hydrazones, with an azomethine -NHN=CH group, are extensively researched due to their easy preparation and numerous pharmaceutical benefits. A hydrazone derivative was formed by combining N,N-dimethyl amino benzaldehyde (**1**) and hydrazine hydrate (**2**), producing-4-(methanehydrazonoyl)-N,N-dimethylaniline (**3**). The final product (H1L) ligand was produced by reacting with ethyl acetate. The new complexes were formed by reacting Co(II), Ni(II), Cu(II), and Zn(II) with the ligand in a 1M:2L molar ratio. Complexes were synthesized with high yields. Metal chelate structures were identified through elemental analyses, FT-IR, magnetic moment, XRD, and molar conductivity tests. According to FT-IR findings, the Schiff base ligand displayed neutral bidentate properties by binding with metal ions via the azomethine N and carbonyl O. Magnetic moment research indicated an octahedral structure and high electrolytic properties, with the exception of Co(II) and Zn(II) complexes, which were observed to be non-electrolytes. Theoretical calculations were performed using DFT. The synthesized complexes were tested for antibacterial activity against two types of Gram-positive bacteria: *S. aureus* and *B. subtilis*. Molecular docking analysis revealed information about the ligand's binding energy and interaction with the *S. aureus* receptor.

KEY WORDS: Hydrazinylidene, DFT, Antibacterial activity, Molecular docking

INTRODUCTION

New complex diseases may develop in humans due to changing global weather conditions. Finding new therapies for diseases caused by pathogenic strains is crucial to improving human life. Numerous substances synthesized or isolated from natural sources have shown significant medicinal potential. Hydrazones, a class of synthetic organic compounds, are gaining recognition in the pharmaceutical industry for their various health benefits. Researchers are exploring the construction of supramolecular inorganic-organic systems using small building blocks like metal ions or salts with ligands. These blocks exhibit specific patterns by interacting via coordination, hydrogen bonding, and π–π interactions [1]. This coordination chemistry produces unique structures of interest. Developing novel antimicrobial drugs with distinct properties is crucial to combat antibacterial resistance. It is important to search for new compounds with potent antibacterial and antifungal qualities, such as hydrazine and its analogs. These compounds have significant pharmacological effects, including scavenging free radicals and combating bacterial strains [2]. Researchers aim to develop novel antimicrobial drugs with distinct chemical properties to address the growing issue of antibacterial resistance. These compounds, including ones with an active site represented by the –HC=N–NH– link, are being investigated for their antibacterial and antifungal properties in coordination chemistry for creating unique structures. In addition, hydrazineylidene and its derivatives have been found to possess significant properties as antibacterial, anticancer, anti-inflammatory, antioxidant, antitumor, antiprotozoal, cardioprotective, antimalarial and antituberculosis agents [3]. There is a major concern for public health due to the rise in multidrug resistance exhibited by various microbes like *Enterococcus*

*Corresponding authors. E-mail: nuha.23scp89@student.uomosul.edu.iq, Sahbaa-ali@uomosul.edu.iq

faecium, *Scedosporium apiospernum*, *Escherichia coli*, *S. epidermidis*, *Pseudomonas aeruginosa*, and *Staphylococcus aureus*. Despite extensive research efforts over the years to discover changes in the structure of existing antibacterial frameworks, the discovery of new antimicrobial compounds remains challenging[4]. Therefore, in the present work, Schiff base ligand (H_1L) was prepared from condensation of 4-(methanehydrazonoyl)-N,N-dimethylaniline with ethyl acetate. The resulting novel Schiff base ligand coordination was investigated with metal ions such as Co(II), Ni(II), Cu(II), and Zn(II) ions.Their corresponding composition was elucidated using various spectral methods, such as IR and ^{1}H NMR. The latter aided the verification of the coordination manner. DFT calculations supported the structural elucidation. Likewise, the antibacterial properties of the Schiff base ligand and its metal chelates were also assessed .Furthermore, simulations of molecular docking were also carried out to try to learn more about the potent antibacterial activity of the produced (H_1L) ligand and the *S. aureus* receptor's binding sites.

EXPERIMENTAL

Chemicals and solvents

Chemicals were purchased from Merck and Sigma-Aldrich and used without further purification. Co(II) chloride, Ni(II) chloride, Zn(II) chloride, Cu(II) chloride, and hydrazine 98%, N,N-dimethylaminobenzdehyde, ethyl acetate were among the compounds used. Organic solvents such as methanol, ethanol, dimethyl sulfoxide (DMSO) and dimethylformamide (DMF) were spectroscopically free from BDH.

Synthesis

H_1L- Schiff base ligand preparation

Step 1. Synthesis of N'-(4-(methanehydrazonoyl)-N,N-dimethylaniline [5]. A mixture of N,N-dimethylaminobenzaldehyde (1g,0.007 mol) and hydrazine hydrate 98% (0.35g, 0.007 mol) was dissolved in ethanol (30 mL) to give a clear solution and refluxed for 5 h. The content was concentrated to half of the volume and allowed to, cool. The solid mass of product, which separated out on cooling was retained by filtering and washed with small amount of ice-cooled ethanol. Yield: 85%, m.p.: 240 °C, give the target compound represented by FT-IR and ^{1}H-NMR in Scheme 1.

Step 2. Synthesis of N'-(4-(dimethylamino)benzylidene)acetohydrazide. A mixture of ethyl acetate (0.8 g , 0.01 mol) and 4-(methanehydrazonoyl)-N,N-dimethylaniline (1.63 g , 0.01 mol) in 25 mL ethanolic medium containing few drops of concentrated HCl was refluxed for 3 h. The product separated on evaporation of the solvent was filterer, washed with alcohol and then finely recrystallized from ethanol, to give the corresponding H_1L ligand pathway is shown in Scheme 1.

Metal chelates preparation

The Schiff base ligand (H_1L) (0.41 g, 0.002 mol) was dissolved in ethanol. The following methanolic metal salt solutions were added to the (H_1L) ligand, solution at the molar ratio (2L:1M): 0.2379 g Co(II), 0.2377,g Ni(II), 0.1704,g Cu (II), and 0.2444,g Zn (II). The mixture was refluxed and stirred for 5 h at 80 °C.The resultant product was filtered and repeatedly cleaned with a water-MeOH solution (1:3). and petroleum,ether, The synthesized complexes were dried in desiccators over anhydrous,$CaCl_2$ in a vacuum desiccator [6], and finally re-crystallized from methanol. Route of synthesis is shown in Scheme 1.

Characterization

The open capillary method was used for the detection of melting points and was uncorrected by Stuart-SMP10. Elemental microanalysis recorder by using the Elementar Vario Micro Cube. ^{1}H NMR spectra were determined on (Bruker Bio Spin GmbH, 400 MHz), tetramethyl silane was used as an internal reference, and chemical shifts are quoted in δ (ppm). X,pert Philips Holland was utilized to obtain XRD patterns, the FT-IR spectrum was recorded reflectively on a spectrophotometer (ATR, Alpha platinum, Bruker) in wave number (400–4000 cm^{-1}), and electrical conductivity measurements of the complexes were recorded at 25 °C, Using a conductivity meter (model 4510–Jenway), measured the samples' (10^{-3} mol.L^{-1}) solutions of the synthesized compounds in DMF were determined using magnetic susceptibility balance Model (MSB_MKI). The electronic spectra were recorded in DMF (UV-Vis) spectrophotometer type UV analytikjenaometer, atomic absorption spectrometry (ICP-AES).

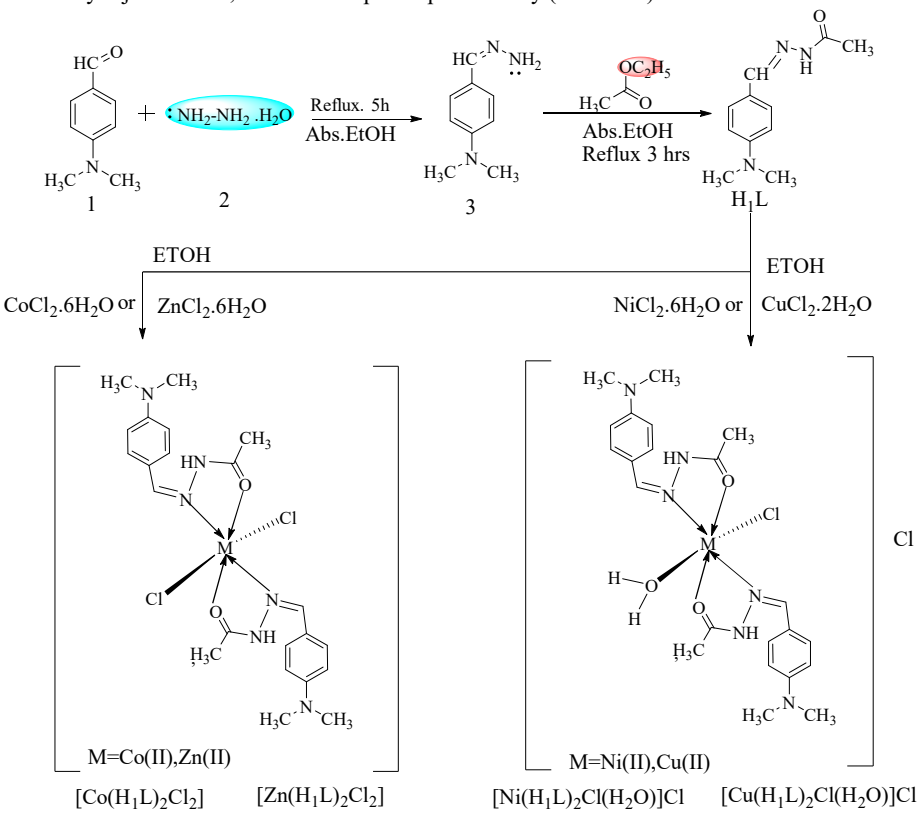

Scheme 1. Preparation of the ligand (H_1L) and corresponding metal complexes.

Powder XRD

X-ray powder data were especially helpful in determining precise cell characteristics when a single crystal was not available. The complex's crystalline structure is confirmed by the diffraction pattern. The Cu(II) and Zn(II) complexes' XRD patterns, which ranged from 10-79° (θ) at a wavelength of 1.54 Å, are shown in Figure 1a,b.

DFT modeling

Sometimes there's no crystal structure, In order to understand further about the molecular structures of the (H_1L) ligand and its complexes, computer investigations were performed. The software 09 W Gaussian was used for geometric optimizations. The complexes singlet ground state molecular geometries in the gas phase were thoroughly optimized at the B3LYP level of theory. In Figure 2, while LANL2DZ [7, 8] was used to model the Co(II), Ni(II), Cu(II), and Zn(II) atoms and ligand atoms were modeled using the 6–311 (d,p) basis set. The compounds during investigation were found to have optimal geometries, and their molecular border orbitals, LUMO (lowest unoccupied molecular orbital) and HOMO (highest occupied molecular orbital), were also identified. Using the HOMO and LUMO energies, the values of chemical hardness (η), softness (σ),electronegativity (χ),energy gap (ΔE)nucleophilicity,(η), maximum electronic charge (ΔN_{max}) and electrophilicity index (ω) were calculated [9, 10]. The results of the calculation are shown in Table 2.

Molecular docking studies

A widely used method to identify structure-based activity interactions is molecular docking. It additionally makes the ability to predict and confirm a small-molecule ligand's binding to specific target protein binding sites. The Auto Dock Vina1.1.2 program was used in this study to study docking. Crystal structure retrieval: We utilized the RCSB Protein Data Bank to obtain the active site crystal structure of the *S. aureus* receptor in order to carry out the docking calculations. For this specific structure, the 1HSK and PDB ID: 1Q1Y. The ChemAxon Marvin Sketch 5.3.735 program was used to create and conform the ligand's three-dimensional structure, which was then saved in the mol2 format. The optimization and energy minimization of the ligand structures were conducted by the Gaussian 09 software. Prior to the docking calculations, all water molecules and the ligand were removed [10, 14, 15]. Analysis of ligand-protein Interaction to analyze the interaction between the ligand and the targeted protein. The results of molecular docking were visualized in (BIOVIA, Discovery Studio, v4.0.100.13345).

Antibacterial activity

The Agar-disc diffusion method was used to evaluate the antibacterial effects of three different substances. In this technique, newly synthesized (H_1L) ligand and its complexes (25 µg/mL and 50 µg/mL of DMSO) were impregnated into a sterile disc measuring 5 mm in diameter made of filter paper (Whatman no. 1), which was then incubated for 12 hours at 37 ºC on a nutrient agar plate. After 12 hours, measurements were made of the inhibition zones surrounding the dried impregnated discs. Each disk was labeled with its unique ID number on the back of the Petri dish [11-13]. In the same experimental conditions, the antibacterial effectiveness of the compounds under investigation. Were evaluated in comparison to the conventional antibiotic Ciprofloxcin 30 µg/mL of DMSO was used as a reference drug for comparison. Table 3 showed of the zone inhibition for H_1L and its complexes against *Staphylococcus aureus*, and *Bacillus subtilis.*

RESULTS AND DISCUSSION

Structure configuration of the ligand

The prepared ligand was characterized using elemental analysis, FT-IR, and ^{1}H-NMR spectra. In the IR spectra of the ligand, the –NH_2 group disappeared, and new bands related to the amide -NH group emerged at around 3391, and C=O group 1624 cm^{-1}. The ^{1}H-NMR spectrum in DMSO-d_6 showed signals for –NH group at δ 11.03 ppm, azomethine -N=CH– group at δ 8.49 ppm,

aromatic proton signals from δ 6.77 to 7.66, and methyl group at 2.99 (s, 3H N-$(CH_3)_2$), 2.25 (s, 3H CH_3) (**5**).

Structure configuration of the complexes

Molar conductance and elemental analysis

The synthesized complexes were soluble in common organic solvents such as DMF, acetone, and DMSO but they were insoluble in water. The findings of the microanalysis for the metal complexes (CHN) showed a good agreement between calculated and observed values, confirming the proposed formula in Table 1. The prepared complexes had low molar conductivity values, indicating they were non-electrolytes except for Ni(II) and Cu(II), as shown in Table 1.

Binding mode and FTIR spectra

The FTIR spectrum data illustrates how ligand interact with metal ions. Comparing IR spectra of metal complexes and free ligand can help identify coordination sites for potential chelation, as shown in Table 1.

Table 1. Physicochemical and spectroscopic date of the prepared ligand and corresponding complexes.

		H_1L	LCo	LNi	LCu	LZn
Color		Yellow	Yellow	Yellowish	Brownish	Yellowish
M.p		230 ºC	240 ºC	252 ºC	268 ºC	250 ºC
Yield		78%	83%	81%	80%	82%
CHN, Found (calc.) %	C	64.54 (64.37)	48.79 (48.90)	47.50 (47.34)	46.98 (46.92)	48.50 (48.32)
	H	7.53 (7.37)	5.79 (5.60)	5.89 (5.78)	5.86 (5.73)	5.68 (5.53)
	N	20.52 (20.47)	15.76 (15.55)	15.25 (15.06)	14.88 (14.93)	15.40 (15.37)
	M	--	10.99 (10.90)	10.62 (10.52)	11.38 (11.29)	11.98 (11.92)
μeff (BM)		--	4.73	3.16	1.78	Diamagnetic
Conductivity	$\Omega^{-1}cm^2mol^{-1}$		15.9	83.8	80.8	13.8
IR spectra	ν (-NH)	3391	3385	3382	3383	3391
	ν (OH_{broad})	--	--	3328	3330	--
	ν (C=O)	1624	1614	1614	1614	1614
	ν (-CH=N)	1587	1564	1564	1564	1561
	N-N	1187	1157	1136	1121	1187
	ν (M-O)	--	641	641	642	641
	ν (M-N)	---	446	446	446	446
UV-Vis	Λ_{max}	270	723 360 287	386 408 730	727	368
Stoichiometry	M : L	--	1:2	1:2	1:2	1:2

Comparing the infrared spectra of the free ligand and its metal complexes allowed investigators to better understand the coordination mode and positions of the ligand to the metal ions. The IR spectra's results are assembled here. The azomethine ν(-C=N) linkage is responsible for the band that the Schiff base ligand (H_1L) shows at (1587 cm^{-1}). This band shifts to lower frequencies in their metal complexes' spectra from (1564-1561 cm^{-1}). The imine nitrogen takes part in chelation with the metal ion [16, 17], based on a comparison between the Schiff base's and

the complexes' IR spectra, Table 1. It is anticipated that the coordination of nitrogen with the metal ion will lower the azomethine link's electron density, shifting the ν(-C=N) group. C=O, shift in band positions confirmed their participation in the bonding to the metal ions. Furthermore, bands found in the complexes between (641-642 cm^{-1}) and (441-446 cm^{-1}), which have been missing in the free ligand are assigned to the ν(M–O) and ν(M–N) vibrations [3, 19]. The appearance of bands belonging to water molecules coordinated with the metal ion in complex LNi and LCu in the region (3328-3445 cm^{-1}). A new band attributed to the symmetric and asymmetric vibration of coordinated water molecules occurred at (960–968 cm^{-1}). The ligand demonstrates neutral bi-dentate behavior with NO donor sites, according to the aforementioned information.

Magnetic measurements and electronic spectra

The UV-Vis spectra of the compounds synthesized exhibit a significant bath chromic shift in the ligand peak, as shown in Table 1. Clear peaks in the metal complexes suggest the formation of complexes with the ligand, with additional peaks indicating a change in electronic configuration when forming complexes, confirming effective bonding between metal ions and the ligand. The presence of new peaks signifies an alteration in the electronic structure of the compounds upon complexation, confirming the successful coordination between metal ions and ligand. One of the best ways to understand the transition metal complexes' structural geometry is to use the effective magnetic moment, μeff = 2.830 (((Xg*Mwt) -(diamagnetic rectification*T))$^{0.5}$ [18, 19]. The electronic scale of the LCo complex, revealed a peak at 723, 360, 287 nm, which is assignable to $^4T_1g(F)\rightarrow{}^4T_2g(F)$, $^4T_1g(F)\rightarrow{}^4T_1g(P)$, $^4T_1g(F)\rightarrow{}^4A_2g(F)$ transitions. The estimated μeff of the LCo complex at 25 °C is 4.73 BM, suggesting the LCo complex has an octahedral geometry, Table 1. The electronic spectrum of the LNi, exhibits bands at 730, 408, 386 nm, which may be related to the $^3A_2g\rightarrow{}^3T_2g$, $^3A_2g\rightarrow{}^3T_1g(F)$, $^3A_2g\rightarrow{}^3T_1g(P)$ transitions, indicating octahedral geometry around the nickel(II) center. The calculated μeff of LNi compound is 3.16 B.M., suggesting the LNi complex has an octahedral geometry, Table 1. The electronic spectrum of the LCu compound, exhibits band at 727 nm, which may be associated to the $^2Eg\rightarrow{}^2T_2g$ transitions, indicating octahedral geometry around the copper (II) center, Table 1. The intended μeff of LCu compound is 1.78 B.M., suggesting the LCu complex has an octahedral geometry, Table 1. The electronic spectrum of the LZn compound, exhibits a band at 368 nm, which might be ascribed to the (L→M). The diamagnetic character of the LZn complex would be attributed to the octahedral geometry of the LZn complex, Table 1.

Interpretation of a complex structure

The analyzed compounds contain C, H, and N in varying proportions. The experimental section displays elemental analyses (C, H, and N) and molecular formulae of the complexes. Metal chelates have a 1:2 metal-ligand ratio, elemental composition, and molar conductivity tests confirmed structures of H_1L ligand with Co(II), Ni(II), Cu(II), and Zn(II) ions. The H_1L ligand binds to cations through (azomethine) nitrogen atom and (carbonyl) oxygen, acting as a bi-dentate neutral ligand. Ni(II) and Cu(II) chelates are electrolytes, Co(II) and Zn(II) chelates are non-electrolytes. Molar conductivity, μeff (B.M.) and UV-Vis spectra suggests an octahedral structure for investigated metal chelates $[Co(H_1L)_2Cl_2]$, $[Ni(H_1L)_2Cl(H_2O)]Cl$, $[Cu(H_1L)_2Cl(H_2O)]Cl$, $[Zn(H_1L)_2Cl_2]$, LCo, LNi, LCu and LZn, complexes correspondingly, Scheme 1.

Powder X-ray diffraction

The XRD pattern of the metal complexes exhibits well-defined crystalline peaks, indicating that the samples were in a crystalline phase. D = Kλ/βCosθ is Scherer's equation, which was used to determine the grain size of the metal Schiff base complexes , where 'β' is the full width at half

maximum of the prominent intensity peak, 'θ' is the diffraction angle, 'λ' is the wavelength, and 'D' is the crystal size rate (nm).The average grain size values for the complexes are (15.65-42.35), (8.11-14.12) nm suggesting that they were in a crystalline regime [10, 20, 21].

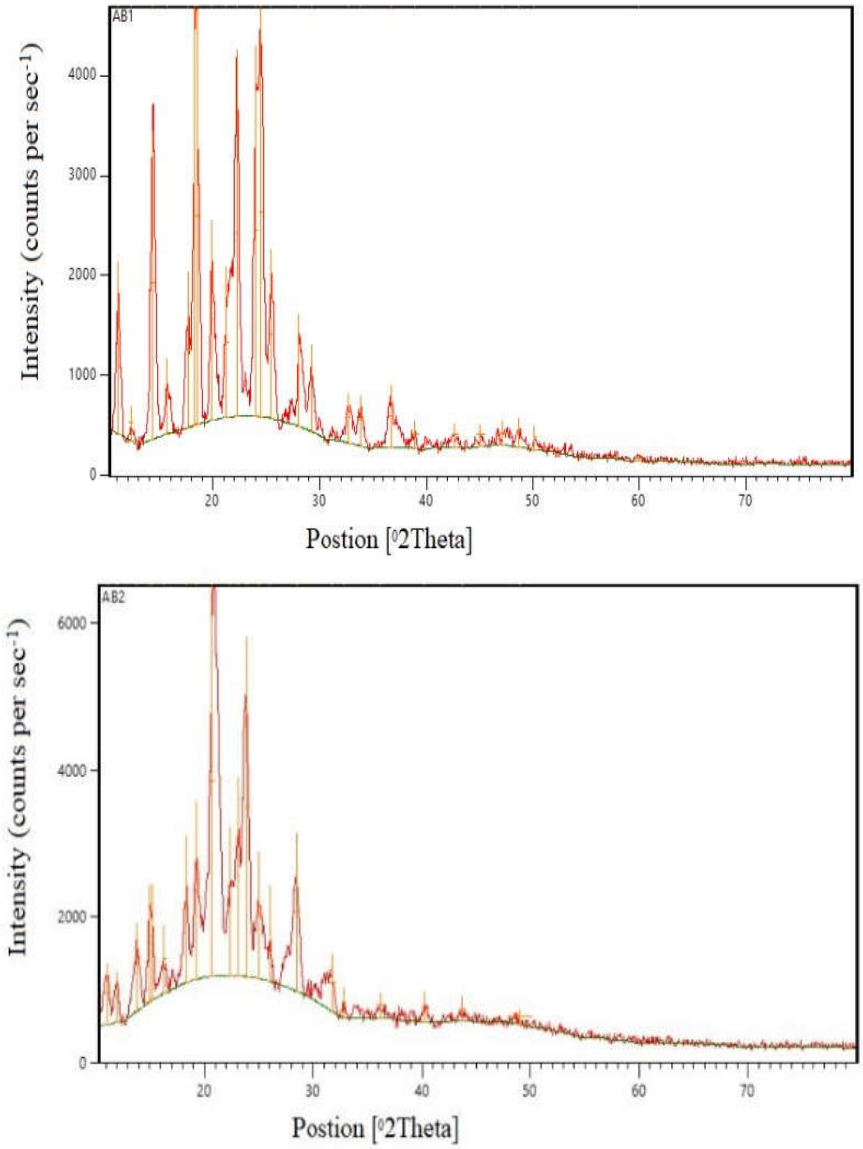

Figure 1. XRD spectra of (a) Cu(II) complex and (b) Zn(II) complex.

DFT calculations

Molecular modeling is becoming more vital for analyzing the structures of coordination compounds when X-ray crystal data is unavailable, offering additional structural information and energy-minimized conformation. The compounds' three-dimensional orbitals, that are the outcome of HOMO and LUMO calculations performed at the DFT/B3LYP level of theory. The energy values of the ligand/metal complexes' HOMO/LUMO are shown in Figure. 3, in eV, with the distribution of the complete molecule's HOMO/LUMO depicted. These molecules have low polarization and are referred to as "hard" molecules when the HOMO-LUMO energy difference is large. Conversely, the molecules are described to as "soft" when there is minimal variation in the HOMO-LUMO energy, strong polarization, and easily influenced electron distribution. The HOMO-LUMO energy gap of the ligand and its metal chelates with Co(II), Ni(II), Cu(II) and Zn(II) ions was calculated to be 6.374, 5.353, 4.651, 2.686 and 0.721 eV, respectively. When compared to the metal complexes, the ligand's HOMO-LUMO energy gap is greater. In terms of energy gaps, the compounds are arranged as follows: L > NiL > CuL > Co > Zn.

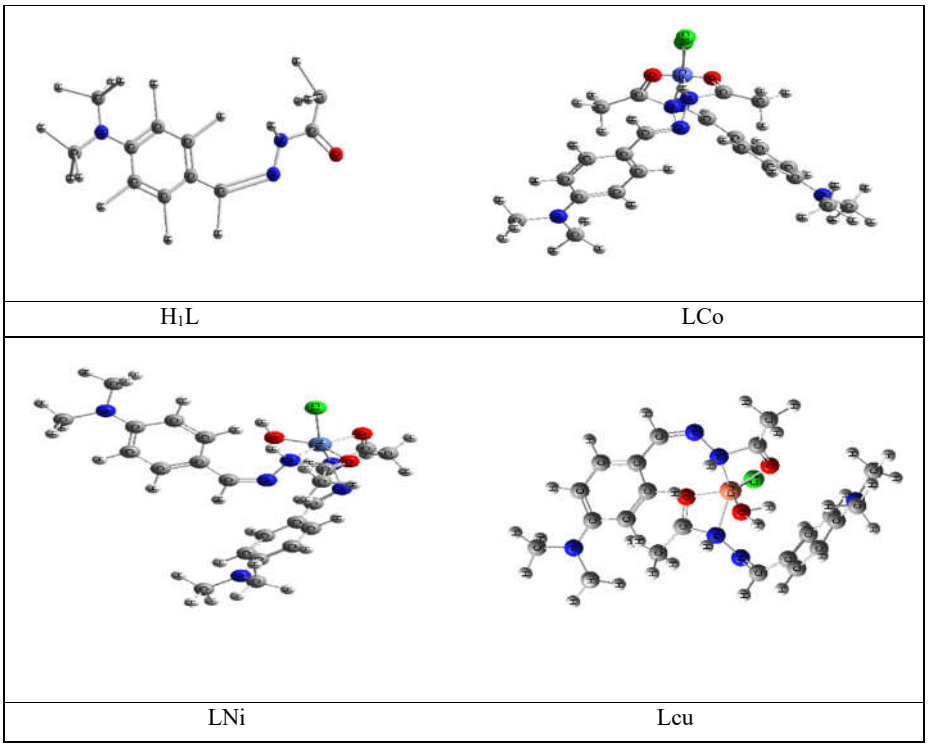

Figure 2. Optimized 3D structure of the ligand and some of its complexes.

Determining absolute hardness (η) and softness (σ) is crucial for understanding molecular stability and reactivity. The ligand's higher binding energy signifies greater stability than the complexes. Additional parameters like Pi, ω, S, χ, and ΔN_{max} were also computed for ligands and their complexes. Analyzing the energy gaps between HOMO and LUMO orbitals provides vital information for assessing molecular hardness and softness. (H_1L) was identified as the most stable

molecule, while (LNi) exhibited the highest reactivity and softness, and (LCu) was considered a neutral molecule. Chemical descriptors like η and σ are used to characterize molecular reactivity, with HOMO and LUMO energies being key in their determination. Table 2 presents the calculated results.

Table 2. The calculated quantum chemical parameters of H1L and its complexes.

Compd.	E LUMO	E HOMO	ΔE	χ	η	σ	ρí	δ	ω	ΔN_{max}
H_1L	-0.545	-6.919	6.374	3.732	3.187	0.3137	-3.732	0.1568	2.1850	1.1710
LCo	-2.407	-5.093	2.686	3.75	1.343	0.744	-3.75	0.3723	5.2354	2.7922
LNi	-0.928	-6.281	5.353	3.6045	2.6765	0.373	-3.6045	0.1868	2.4271	1.3467
LCu	-1.049	-5.700	4.651	3.3745	2.3255	0.4300	-3.3745	0.2192	2.4483	1.4510
LZn	-0.813	-1.534	0.721	1.1735	0.3605	2.7739	-1.1735	1.3869	1.9099	3.2552

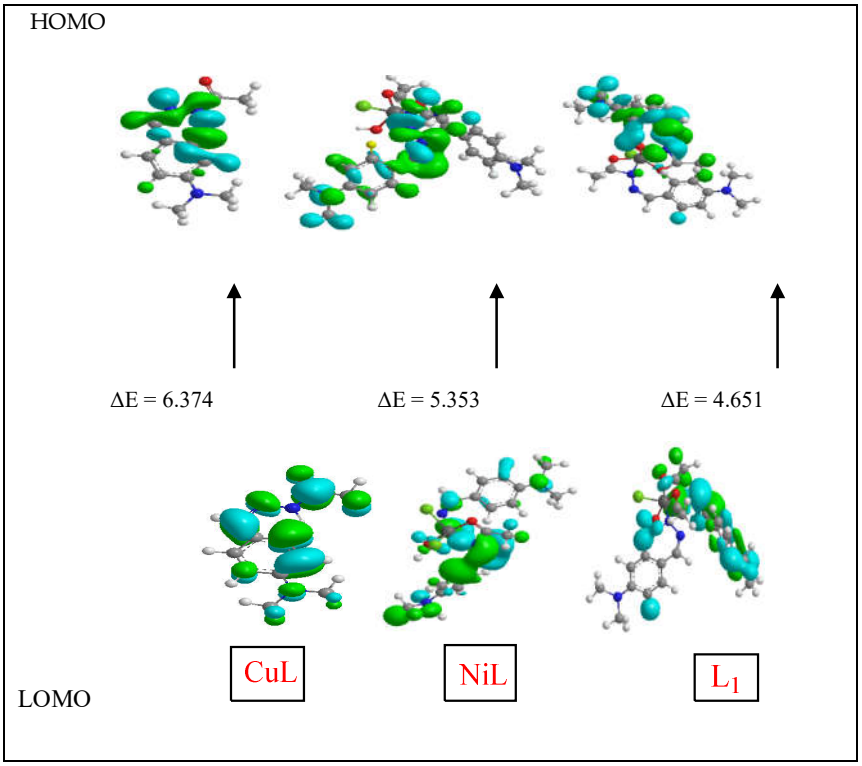

Figure 3. The HOMO and LUMO of the ligands H_1L its NiL and CuL complexes.

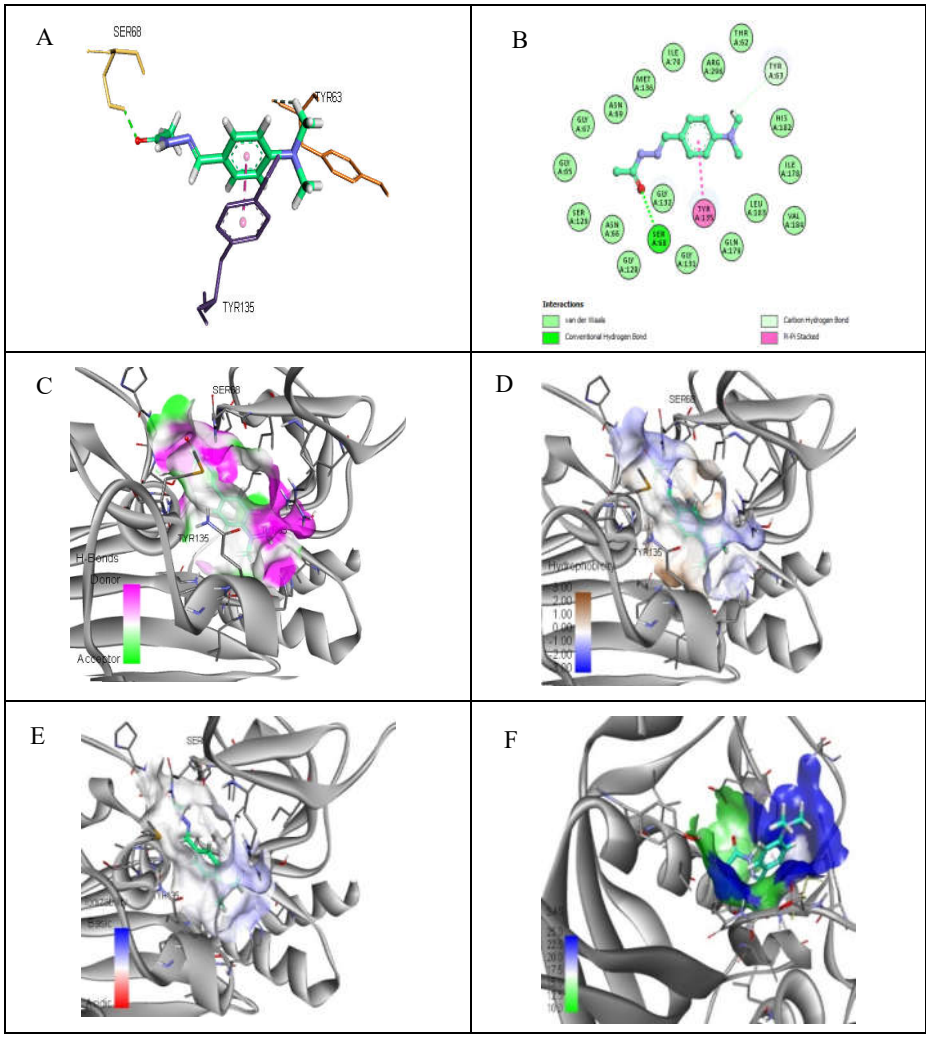

Figure 4. (A) 3D diagrams visualize interactions of (H_1L) with receptor ID: 1HSK of *S. aureus*. (B) 2D diagrams interactions of (H_1L) with receptor ID: 1HSK of *S. aureus*. (C) Represent positions of hydrogen bond between receptor ID: display 1HSK of *S. aureus* and (H_1L). (D) Display positions of hydrophobicity between enzyme and (H_1L) in ID: 1HSK of *S. aureus*. (E) Show interpolated charge between ID: 1HSK of *S. aureus* and (H_1L). (F) Demonstrate susceptibility regions for ID: 1HSK protein interaction with (H_1L).

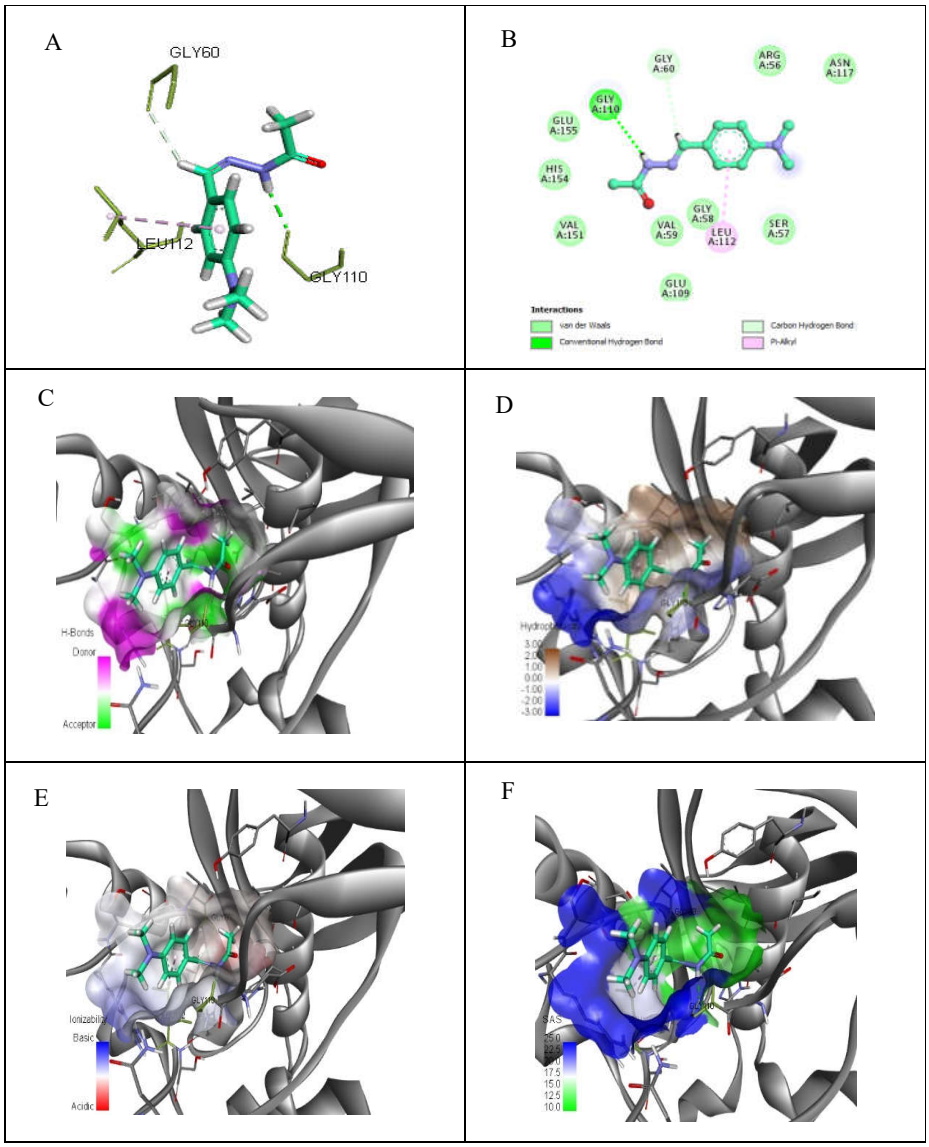

Figure 5. (A) 3D diagrams visualize interactions of (H_1L) with receptor ID: 1Q1Y of *S. aureus*. (B) 2D diagrams display interactions of (H_1L) with receptor ID: 1Q1Y of *S. aureus*. (C) Represent positions of hydrogen bond between receptor ID: 1Q1Y of *S. aureus* and (H_1L). (D) Display positions of hydrophobicity between enzyme and (H_1L) in ID: 1Q1Y of *S. aureus*. (E) Show interpolated charge between ID: 1Q1Y of *S. aureus* and (H_1L). (F) Demonstrate susceptibility regions for ID: 1Q1Y protein interaction with (H_1L).

Molecular docking studies

Molecular docking is a crucial method in designing drug structures, providing valuable insight into ligand-receptor interactions to enhance the drug discovery process. Our approach accuratelypredicts binding affinities and conformations of various species with target proteins[7, 13]. This study focused on the H_1L ligand interaction with the *S. aureus* receptor's active site, highlighting its potential for novel antibiotics. The energy values of the ligand-protein binding determined the effectiveness of docking, with more negative values indicating stronger interactions. Evaluation of binding scores from H_1L ligand-receptor interactions revealed steady attachment to hydrophobic surfaces on proteins, with specific amino acid regions like GLY:132 and TYR:63 and hydrogen bond SER:68,another interaction such as van der Waals for ID: 1HSK receptor. The interaction at PDB ID: 1Q1Y also showed strong binding energies with GLY60, LEU112, and shorter hydrogen bond GLY110, another interaction such as van der Waals on the protein's hydrophobic surface. The binding energy values revealed the ligand's ability to dock with the protein. The H_1L molecule showed stable interactions with specific amino acid regions of the receptors ID: 1HSK and PDB ID: 1Q1Y, with binding energies of -7.00 kcal/mol and -5.90 kcal/mol, respectively. Figures 4 and 5 display the data gathered from the molecular docking study.

Antibacterial activity

The biological properties of complexes are influenced by factors such as the ligand's chelating nature, the type and number of donor atoms, the overall charge of the complex, the specific metal ion present, the chemical composition of the counter ions, and the geometrical arrangement of the complex [13, 15, 22]. Incorporating an azomethine group with chelating properties can significantly enhance the antibacterial effectiveness of Schiff base compounds. This feature enables them to selectively bind to specific sites on bacterial cells, preventing their proliferation, or facilitate the transportation of metals across bacterial membranes. Additionally, the H_1L ligand, Co(II), Ni(II), Cu(II) and Zn(II) metal chelate exhibited antibacterial potential against *S. aureus* and *B. Subtilis* Furthermore, the Ni(II), Cu(II) complexes demonstrated higher antibacterial activity against *B. Subtilis* and *S. aureus*, while the Zn(II) complex showed the lowest antibacterial activity. Moreover, H_1L exhibited the most promising antibacterial activity against both types of bacteria.

Table 3. Inhibition zone of the synthesized compounds (μg/mL).

Compounds	Concentration (μg/mL)	Zone of inhibition (mm)	
		S. aureus	*B. subtilis*
H_1L	50	16.0	13.0
	25	14.9	12.2
CoL	50	14.9	12.0
	25	14.4	11.8
NiL	50	15.8	12.8
	25	15.2	12.2
CuL	50	15.4	12.6
	25	15.0	12.2
ZnL	50	10.8	8.8
	25	10.2	8.0
Ciprodar (+ve control)	30	18	17

CONCLUSION

Four new LCo, LNi, LCu, and LZn complexes were created in this study. The synthesis and characterization of Schiff bases produced from N'-(4-(dimethylamino)benzylidene) acetohydrazide, and physicochemical and spectroscopic methods were used to characterize their structures. According to the results, the H1L ligand acts as a neutral and bi-dentate N and O ligand, binding with Co(II), Cu(II), Ni(II), and Zn(II) in a 1:2 molar ratio. The complexes exhibited octahedral geometry, as indicated by spectral and analytical data. The crystalline structures of Cu(II) and Zn(II) complexes were examined using XRD data. To gain further insights into the molecular properties, DFT with the B3LYP method was employed to predict the optimal geometries and frontier molecular orbitals of the complexes. In vitro tests were conducted to evaluate the antibacterial activity of the ligand and their complexes against pathogenic bacteria. The results of the antibacterial tests indicate that the free ligand exhibits more antibacterial activity than the complexes. Furthermore, molecular docking was applied to determine the bonding interaction between the H1L ligand and the Staphylococcus aureus receptor (PDB ID: 1HSK and ID:1Q1Y). The active region was investigated using a molecular docking approach.

ACKNOWLEDGMENTS

The authors are thankful to the University of Mosul, Department of Chemistry, College of Science, for their support and providing the research facilities to complete this work.

REFERENCES

1. Pyykkö, P. Strong closed-shell interactions in inorganic chemistry. *Chem. Rev.* 1**997**, 97, 597-636.
2. Piotr, P.; Adam, H.; Krystian, P.; Bogumił, B.; Franz, B. Biological properties of schiff bases and azo derivatives of phenols. *Curr. Org. Chem.* **2009**,13, 124-148.
3. Shah, M.A.; Uddin, A.; Shah, M.R.; Ali, I.; Ullah, R.; Hannan, P.A.; Hussain, H. Synthesis and characterization of novel hydrazone derivatives of isonicotinic hydrazide and their evaluation for antibacterial and cytotoxic potential. *Molecules* **2022**, 27, 6770.
4. Youssef, H.M.; Abdulhamed, Y.Kh.; AbuEL-Reash, G.M.. Cr(III) and Ni(II) complexes of isatin-hydrazone ligand: Preparation, characterization, DFT studies, biological activity, and ion-flotation separation of Ni(II). *Inorg. Chem. Commun*. **2022**, 138,109278.
5. Li, W.W.; Yu, T.M.; Yu, W.B.; Lv, L.P.; Hu, X.C. N′-[4-(Dimethylamino) benzylidene] acetohydrazide. *Acta Crystallogr. Sect. E Struct. Rep. Online* **2009**, 65, o2197-o2197.
6. Kriza, A.; Dianu, M.L.; Stanica, N.; Draghici, C.; Popoiu, M. Synthesis and characterization of some tranzition metals complexes with glyoxal bis-isonicotinoyl hydrazone. *Rev. Chim*. **2009**, 60, 555-607.
7. Abd El-Lateef, H.M.; Khalaf, M.M.; Kandeel, M.; Abdou, A. Synthesis, characterization, DFT, biological and molecular docking of mixed ligand complexes of Ni(II), Co(II), and Cu(II) based on ciprofloxacin and 2-(1H-benzimidazol-2-yl) phenol. *Inorg. Chem. Commun.* **2023**, 155, 111087.
8. Abdou, A. Synthesis, structural, molecular docking, DFT, vibrational spectroscopy, HOMO-LUMO, MEP exploration, antibacterial and antifungal activity of new Fe(III), Co(II) and Ni(II) hetero-ligand complexes. *J. Mol. Struct*. **2022**, 1262, 132911.
9. Abu-Dief, A.M.; Alotaibi, N.H.; Al-Farraj, E.; Qasem, H.A.; Alzahrani, S.O.; Mahfouze, M.K.; Abdou, A. Fabrication, structural elucidation, theoretical, TD-DFT, vibrational calculation and molecular docking studies of some novel adenine imine chelates for biomedical applications. *J. Mol. Liq*. **2022**, 365, 119961.

10. Mohamed, G.G.; Mahmoud, W.H.; Refaat, A.M. Nano-azo ligand and its superhydrophobic complexes: Synthesis, characterization, DFT, contact angle, molecular docking, and antimicrobial studies. *J. Chem*. **2020**, 2020, 19.
11. Startseva, Y.D.; Hodyna, D.M.; Semenyuta, I.V.; Tarasyuk, O.P.; Rogalsky, S.P.; Metelytsia, L.O. Undecylenic acid and N,N-dibutylundecenamide as effective antibacterials against antibiotic-resistant strains. *Ukr. Biochem. J.* **2023**, 95, 55-63.
12. Vashistha, V.K.; Mittal, A.; Bala, R.; Das, D.K.; Singh, P.P. Synthesis, characterization, electrochemical and antibacterial studies of MN4-type macrocyclic complexes of Ni(II). *Rev. Roum. Chim*. **2023**, 68, 447-452.
13. Tolan, D.A.; Kashar, T.I.; Yoshizawa, K.; El-Nahas, A.M. Synthesis, spectral characterization, density functional theory studies, and biological screening of some transition metal complexes of a novel hydrazide–hydrazone ligand of isonicotinic acid. *Appl. Organomet. Chem.* **2021**, 35, e6205.
14. Ifeanyichukwu, I.; Eunice, E.U.; Ajoko, I.T.; Jim-Halliday, T.T. Molecular docking, synthesis and antimicrobial evaluation of 4-[(3-hydroxybenzalidene) amino] antipyrine and its copper complex. *Sch. Int. J. Chem. Mater Sci*. **2023**, 6, 149-162.
15. Salih, M.M.; Saleh, A.M.; Hamad, A.S.; Al-Janabi, A.S.M. Synthesis, spectroscopic, anti-bacterial activity, molecular docking, ADMET, toxicity and DNA binding studies of divalent metal complexes of pyrazole-3-one azo ligand. *J. Mol. Struct*. **2022**, 1264, 133252.
16. Hofmeister, A.M. *Infrared Microspectroscopy. Practical Guide to Infrared Spectroscopy*, , Marcel Dekker, Inc.: New York; **1995**; pp. 377-416.
17. Shahab, S.; Sheikhi, M.; Filippovich, L.; Ihnatovich, Z.; Koroleva, E.; Drachilovskaya, M.; Atroshko, M.; Pazniak, A. Spectroscopic (FT-IR, excited states, UV/Vis, polarization) properties, synthesis and quantum chemical studies of new azomethine derivatives. *Dyes Pigm*. **2019**, 170, 107647.
18. Bennour, H.A.; Elmagbari, F.M.; Hammouda, A.N.; EL-Ferjani, R.M.; Amer, Y.O.B.; Soliman, S.M.; Jackson, G.E. Synthesis, characterisation and density functional theory (DFT) studies of a triazine ring with a mixed ligand Schiff base complex. *Results Chem*. **2023**, 5, 100775.
19. Suresh, M.S.; Pracash, V. Preparation and characterization of Cr(III), Mn(II), Co(III), Ni(II), Cu(II), Zn(II) and Cd(II) chelates of Schiff's base derived from vanillin and 4-aminoantipyrine. *Int. Phys. Sci*. **2010**, 5, 2203-221.
20. Jones, R.C.; Malik, H.U. Analysis of minerals in oxide-rich soils by X-ray diffraction. Quantitative methods in soil mineralogy, SSSA: Madison, WI 53711, USA; **1994**; pp. 296-329.
21. Ahmed, I.S.; Moustafa, M.M.; Abd El Aziz, M.M. Mono and binuclear Ag(I), Cu(II), Zn(II) and Hg(II) complexes of a new azo-azomethine as ligand: Synthesis, potentiometric, spectral and thermal studies. *Spectrochim. Acta. A Mol. Biomol. Spectrosc*. **2011**, 78, 1429-1436.
22. Singh, J.; Singh, P. Synthesis, spectroscopic characterization, and in vitro antimicrobial studies of pyridine-2-carboxylic acid N [variant prime]-(4-chloro-benzoyl)-hydrazide and its Co(II), Ni(II), and Cu(II) Complexes. *Bioinorg. Chem. Appl.* **2012**, 2012, 104549.